Study of $e^+e^- \to \gamma\omega J/\psi$ and Observation of $X(3872) \to \omega J/\psi$

M. Ablikim,[1] M. N. Achasov,[10,d] P. Adlarson,[59] S. Ahmed,[15] M. Albrecht,[4] M. Alekseev,[58a,58c] A. Amoroso,[58a,58c] F. F. An,[1] Q. An,[55,43] Y. Bai,[42] O. Bakina,[27] R. Baldini Ferroli,[23a] Y. Ban,[35] K. Begzsuren,[25] J. V. Bennett,[5] N. Berger,[26] M. Bertani,[23a] D. Bettoni,[24a] F. Bianchi,[58a,58c] J. Biernat,[59] J. Bloms,[52] I. Boyko,[27] R. A. Briere,[5] H. Cai,[60] X. Cai,[1,43] A. Calcaterra,[23a] G. F. Cao,[1,47] N. Cao,[1,47] S. A. Cetin,[46b] J. Chai,[58c] J. F. Chang,[1,43] W. L. Chang,[1,47] G. Chelkov,[27,b,c] D. Y. Chen,[6] G. Chen,[1] H. S. Chen,[1,47] J. C. Chen,[1] M. L. Chen,[1,43] S. J. Chen,[33] Y. B. Chen,[1,43] W. Cheng,[58c] G. Cibinetto,[24a] F. Cossio,[58c] X. F. Cui,[34] H. L. Dai,[1,43] J. P. Dai,[38,h] X. C. Dai,[1,47] A. Dbeyssi,[15] D. Dedovich,[27] Z. Y. Deng,[1] A. Denig,[26] I. Denysenko,[27] M. Destefanis,[58a,58c] F. De Mori,[58a,58c] Y. Ding,[31] C. Dong,[34] J. Dong,[1,43] L. Y. Dong,[1,47] M. Y. Dong,[1,43,47] Z. L. Dou,[33] S. X. Du,[63] J. Z. Fan,[45] J. Fang,[1,43] S. S. Fang,[1,47] Y. Fang,[1] R. Farinelli,[24a,24b] L. Fava,[58b,58c] F. Feldbauer,[4] G. Felici,[23a] C. Q. Feng,[55,43] M. Fritsch,[4] C. D. Fu,[1] Y. Fu,[1] Q. Gao,[1] X. L. Gao,[55,43] Y. Gao,[45] Y. Gao,[56] Y. G. Gao,[6] Z. Gao,[55,43] B. Garillon,[26] I. Garzia,[24a] E. M. Gersabeck,[50] A. Gilman,[51] K. Goetzen,[11] L. Gong,[34] W. X. Gong,[1,43] W. Gradl,[26] M. Greco,[58a,58c] L. M. Gu,[33] M. H. Gu,[1,43] S. Gu,[2] Y. T. Gu,[13] A. Q. Guo,[22] L. B. Guo,[32] R. P. Guo,[36] Y. P. Guo,[26] A. Guskov,[27] S. Han,[60] X. Q. Hao,[16] F. A. Harris,[48] K. L. He,[1,47] F. H. Heinsius,[4] T. Held,[4] Y. K. Heng,[1,43,47] Y. R. Hou,[47] Z. L. Hou,[1] H. M. Hu,[1,47] J. F. Hu,[38,h] T. Hu,[1,43,47] Y. Hu,[1] G. S. Huang,[55,43] J. S. Huang,[16] X. T. Huang,[37] X. Z. Huang,[33] N. Huesken,[52] T. Hussain,[57] W. Ikegami Andersson,[59] W. Imoehl,[22] M. Irshad,[55,43] Q. Ji,[1] Q. P. Ji,[16] X. B. Ji,[1,47] X. L. Ji,[1,43] H. L. Jiang,[37] X. S. Jiang,[1,43,47] X. Y. Jiang,[34] J. B. Jiao,[37] Z. Jiao,[18] D. P. Jin,[1,43,47] S. Jin,[33] Y. Jin,[49] T. Johansson,[59] N. Kalantar-Nayestanaki,[29] X. S. Kang,[31] R. Kappert,[29] M. Kavatsyuk,[29] B. C. Ke,[1] I. K. Keshk,[4] T. Khan,[55,43] A. Khoukaz,[52] P. Kiese,[26] R. Kiuchi,[1] R. Kliemt,[11] L. Koch,[28] O. B. Kolcu,[46b,f] B. Kopf,[4] M. Kuemmel,[4] M. Kuessner,[4] A. Kupsc,[59] M. Kurth,[1] M. G. Kurth,[1,47] W. Kühn,[28] J. S. Lange,[28] P. Larin,[15] L. Lavezzi,[58c] H. Leithoff,[26] T. Lenz,[26] C. Li,[59] Cheng Li,[55,43] D. M. Li,[63] F. Li,[1,43] F. Y. Li,[35] G. Li,[1] H. B. Li,[1,47] H. J. Li,[9,j] J. C. Li,[1] J. W. Li,[41] Ke Li,[1] L. K. Li,[1] Lei Li,[3] P. L. Li,[55,43] P. R. Li,[30] Q. Y. Li,[37] W. D. Li,[1,47] W. G. Li,[1] X. H. Li,[55,43] X. L. Li,[37] X. N. Li,[1,43] X. Q. Li,[34] Z. B. Li,[44] H. Liang,[1,47] H. Liang,[55,43] Y. F. Liang,[40] Y. T. Liang,[28] G. R. Liao,[12] L. Z. Liao,[1,47] J. Libby,[21] C. X. Lin,[44] D. X. Lin,[15] Y. J. Lin,[13] B. Liu,[38,h] B. J. Liu,[1] C. X. Liu,[1] D. Liu,[55,43] D. Y. Liu,[38,h] F. H. Liu,[39] Fang Liu,[1] Feng Liu,[6] H. B. Liu,[13] H. M. Liu,[1,47] Huanhuan Liu,[1] Huihui Liu,[17] J. B. Liu,[55,43] J. Y. Liu,[1,47] K. Y. Liu,[31] Ke Liu,[6] Q. Liu,[47] S. B. Liu,[55,43] T. Liu,[1,47] X. Liu,[30] X. Y. Liu,[1,47] Y. B. Liu,[34] Z. A. Liu,[1,43,47] Zhiqing Liu,[37,*] Y. F. Long,[35] X. C. Lou,[1,43,47] H. J. Lu,[18] J. D. Lu,[1,47] J. G. Lu,[1,43] Y. Lu,[1] Y. P. Lu,[1,43] C. L. Luo,[32] M. X. Luo,[62] P. W. Luo,[44] T. Luo,[9,j] X. L. Luo,[1,43] S. Lusso,[58c] X. R. Lyu,[47] F. C. Ma,[31] H. L. Ma,[1] L. L. Ma,[37] M. M. Ma,[1,47] Q. M. Ma,[1] X. N. Ma,[34] X. X. Ma,[1,47] X. Y. Ma,[1,43] Y. M. Ma,[37] F. E. Maas,[15] M. Maggiora,[58a,58c] S. Maldaner,[26] S. Malde,[53] Q. A. Malik,[57] A. Mangoni,[23b] Y. J. Mao,[35] Z. P. Mao,[1] S. Marcello,[58a,58c] Z. X. Meng,[49] J. G. Messchendorp,[29] G. Mezzadri,[24a] J. Min,[1,43] T. J. Min,[33] R. E. Mitchell,[22] X. H. Mo,[1,43,47] Y. J. Mo,[6] C. Morales Morales,[15] N. Yu. Muchnoi,[10,d] H. Muramatsu,[51] A. Mustafa,[4] S. Nakhoul,[11,g] Y. Nefedov,[27] F. Nerling,[11,g] I. B. Nikolaev,[10,d] Z. Ning,[1,43] S. Nisar,[8,k] S. L. Niu,[1,43] S. L. Olsen,[47] Q. Ouyang,[1,43,47] S. Pacetti,[23b] Y. Pan,[55,43] M. Papenbrock,[59] P. Patteri,[23a] M. Pelizaeus,[4] H. P. Peng,[55,43] K. Peters,[11,g] J. Pettersson,[59] J. L. Ping,[32] R. G. Ping,[1,47] A. Pitka,[4] R. Poling,[51] V. Prasad,[55,43] M. Qi,[33] T. Y. Qi,[2] S. Qian,[1,43] C. F. Qiao,[47] N. Qin,[60] X. P. Qin,[13] X. S. Qin,[4] Z. H. Qin,[1,43] J. F. Qiu,[1] S. Q. Qu,[34] K. H. Rashid,[57,i] K. Ravindran,[21] C. F. Redmer,[26] M. Richter,[4] M. Ripka,[26] A. Rivetti,[58c] V. Rodin,[29] M. Rolo,[58c] G. Rong,[1,47] Ch. Rosner,[15] M. Rump,[52] A. Sarantsev,[27,e] M. Savri,[24b] K. Schoenning,[59] W. Shan,[19] X. Y. Shan,[55,43] M. Shao,[55,43] C. P. Shen,[2] P. X. Shen,[34] X. Y. Shen,[1,47] H. Y. Sheng,[1] X. Shi,[1,43] X. D. Shi,[55,43] J. J. Song,[37] Q. Q. Song,[55,43] X. Y. Song,[1] S. Sosio,[58a,58c] C. Sowa,[4] S. Spataro,[58a,58c] F. F. Sui,[37] G. X. Sun,[1] J. F. Sun,[16] L. Sun,[60] S. S. Sun,[1,47] X. H. Sun,[1] Y. J. Sun,[55,43] Y. K. Sun,[55,43] Y. Z. Sun,[1] Z. J. Sun,[1,43] Z. T. Sun,[1] Y. T. Tan,[55,43] C. J. Tang,[40] G. Y. Tang,[1] X. Tang,[1] V. Thoren,[59] B. Tsednee,[25] I. Uman,[46d] B. Wang,[1] B. L. Wang,[47] C. W. Wang,[33] D. Y. Wang,[35] H. H. Wang,[37] K. Wang,[1,43] L. L. Wang,[1] L. S. Wang,[1] M. Wang,[37] M. Z. Wang,[35] Meng Wang,[1,47] P. L. Wang,[1] R. M. Wang,[61] W. P. Wang,[55,43] X. Wang,[35] X. F. Wang,[1] X. L. Wang,[9,j] Y. Wang,[55,43] Y. F. Wang,[1,43,47] Z. Wang,[1,43] Z. G. Wang,[1,43] Z. Y. Wang,[1] Zongyuan Wang,[1,47] T. Weber,[4] D. H. Wei,[12] P. Weidenkaff,[26] H. W. Wen,[32] S. P. Wen,[1] U. Wiedner,[4] G. Wilkinson,[53] M. Wolke,[59] L. H. Wu,[1] L. J. Wu,[1,47] Z. Wu,[1,43] L. Xia,[55,43] Y. Xia,[20] S. Y. Xiao,[1] Y. J. Xiao,[1,47] Z. J. Xiao,[32] Y. G. Xie,[1,43] Y. H. Xie,[6] T. Y. Xing,[1,47] X. A. Xiong,[1,47] Q. L. Xiu,[1,43] G. F. Xu,[1] J. J. Xu,[33] L. Xu,[1] Q. J. Xu,[14] W. Xu,[1,47] X. P. Xu,[41] F. Yan,[56] L. Yan,[58a,58c] W. B. Yan,[55,43] W. C. Yan,[2] Y. H. Yan,[20] H. J. Yang,[38,h] H. X. Yang,[1] L. Yang,[60] R. X. Yang,[55,43] S. L. Yang,[1,47] Y. H. Yang,[33] Y. X. Yang,[12] Yifan Yang,[1,47] Z. Q. Yang,[20] M. Ye,[1,43] M. H. Ye,[7] J. H. Yin,[1] Z. Y. You,[44] B. X. Yu,[1,43,47] C. X. Yu,[34] J. S. Yu,[20] C. Z. Yuan,[1,47] X. Q. Yuan,[35] Y. Yuan,[1] A. Yuncu,[46b,a] A. A. Zafar,[57] Y. Zeng,[20] B. X. Zhang,[1] B. Y. Zhang,[1,43] C. C. Zhang,[1] D. H. Zhang,[1] H. H. Zhang,[44] H. Y. Zhang,[1,43] J. Zhang,[1,47] J. L. Zhang,[61] J. Q. Zhang,[4] J. W. Zhang,[1,43,47] J. Y. Zhang,[1] J. Z. Zhang,[1,47]

K. Zhang,[1,47] L. Zhang,[45] S. F. Zhang,[33] T. J. Zhang,[38,h] X. Y. Zhang,[37] Y. Zhang,[55,43] Y. H. Zhang,[1,43] Y. T. Zhang,[55,43] Yang Zhang,[1] Yao Zhang,[1] Yi Zhang,[9,j] Yu Zhang,[47] Z. H. Zhang,[6] Z. P. Zhang,[55] Z. Y. Zhang,[60] G. Zhao,[1] J. W. Zhao,[1,43] J. Y. Zhao,[1,47] J. Z. Zhao,[1,43] Lei Zhao,[55,43] Ling Zhao,[1] M. G. Zhao,[34] Q. Zhao,[1] S. J. Zhao,[63] T. C. Zhao,[1] Y. B. Zhao,[1,43] Z. G. Zhao,[55,43] A. Zhemchugov,[27,b] B. Zheng,[56] J. P. Zheng,[1,43] Y. Zheng,[35] Y. H. Zheng,[47] B. Zhong,[32] L. Zhou,[1,43] L. P. Zhou,[1,47] Q. Zhou,[1,47] X. Zhou,[60] X. K. Zhou,[47] X. R. Zhou,[55,43] Xiaoyu Zhou,[20] Xu Zhou,[20] A. N. Zhu,[1,47] J. Zhu,[34] J. Zhu,[44] K. Zhu,[1] K. J. Zhu,[1,43,47] S. H. Zhu,[54] W. J. Zhu,[34] X. L. Zhu,[45] Y. C. Zhu,[55,43] Y. S. Zhu,[1,47] Z. A. Zhu,[1,47] J. Zhuang,[1,43] B. S. Zou,[1] and J. H. Zou[1]

(BESIII Collaboration)

[1]Institute of High Energy Physics, Beijing 100049, People's Republic of China
[2]Beihang University, Beijing 100191, People's Republic of China
[3]Beijing Institute of Petrochemical Technology, Beijing 102617, People's Republic of China
[4]Bochum Ruhr-University, D-44780 Bochum, Germany
[5]Carnegie Mellon University, Pittsburgh, Pennsylvania 15213, USA
[6]Central China Normal University, Wuhan 430079, People's Republic of China
[7]China Center of Advanced Science and Technology, Beijing 100190, People's Republic of China
[8]COMSATS University Islamabad, Lahore Campus, Defence Road, Off Raiwind Road, 54000 Lahore, Pakistan
[9]Fudan University, Shanghai 200443, People's Republic of China
[10]G.I. Budker Institute of Nuclear Physics SB RAS (BINP), Novosibirsk 630090, Russia
[11]GSI Helmholtzcentre for Heavy Ion Research GmbH, D-64291 Darmstadt, Germany
[12]Guangxi Normal University, Guilin 541004, People's Republic of China
[13]Guangxi University, Nanning 530004, People's Republic of China
[14]Hangzhou Normal University, Hangzhou 310036, People's Republic of China
[15]Helmholtz Institute Mainz, Johann-Joachim-Becher-Weg 45, D-55099 Mainz, Germany
[16]Henan Normal University, Xinxiang 453007, People's Republic of China
[17]Henan University of Science and Technology, Luoyang 471003, People's Republic of China
[18]Huangshan College, Huangshan 245000, People's Republic of China
[19]Hunan Normal University, Changsha 410081, People's Republic of China
[20]Hunan University, Changsha 410082, People's Republic of China
[21]Indian Institute of Technology Madras, Chennai 600036, India
[22]Indiana University, Bloomington, Indiana 47405, USA
[23a]INFN Laboratori Nazionali di Frascati, I-00044 Frascati, Italy
[23b]INFN and University of Perugia, I-06100 Perugia, Italy
[24a]INFN Sezione di Ferrara, I-44122 Ferrara, Italy
[24b]University of Ferrara, I-44122 Ferrara, Italy
[25]Institute of Physics and Technology, Peace Ave. 54B, Ulaanbaatar 13330, Mongolia
[26]Johannes Gutenberg University of Mainz, Johann-Joachim-Becher-Weg 45, D-55099 Mainz, Germany
[27]Joint Institute for Nuclear Research, 141980 Dubna, Moscow region, Russia
[28]Justus-Liebig-Universitaet Giessen, II. Physikalisches Institut, Heinrich-Buff-Ring 16, D-35392 Giessen, Germany
[29]KVI-CART, University of Groningen, NL-9747 AA Groningen, Netherlands
[30]Lanzhou University, Lanzhou 730000, People's Republic of China
[31]Liaoning University, Shenyang 110036, People's Republic of China
[32]Nanjing Normal University, Nanjing 210023, People's Republic of China
[33]Nanjing University, Nanjing 210093, People's Republic of China
[34]Nankai University, Tianjin 300071, People's Republic of China
[35]Peking University, Beijing 100871, People's Republic of China
[36]Shandong Normal University, Jinan 250014, People's Republic of China
[37]Shandong University, Jinan 250100, People's Republic of China
[38]Shanghai Jiao Tong University, Shanghai 200240, People's Republic of China
[39]Shanxi University, Taiyuan 030006, People's Republic of China
[40]Sichuan University, Chengdu 610064, People's Republic of China
[41]Soochow University, Suzhou 215006, People's Republic of China
[42]Southeast University, Nanjing 211100, People's Republic of China
[43]State Key Laboratory of Particle Detection and Electronics, Beijing 100049, Hefei 230026, People's Republic of China
[44]Sun Yat-Sen University, Guangzhou 510275, People's Republic of China
[45]Tsinghua University, Beijing 100084, People's Republic of China
[46a]Ankara University, 06100 Tandogan, Ankara, Turkey
[46b]Istanbul Bilgi University, 34060 Eyup, Istanbul, Turkey

[46c]*Uludag University, 16059 Bursa, Turkey*
[46d]*Near East University, Nicosia, North Cyprus, Mersin 10, Turkey*
[47]*University of Chinese Academy of Sciences, Beijing 100049, People's Republic of China*
[48]*University of Hawaii, Honolulu, Hawaii 96822, USA*
[49]*University of Jinan, Jinan 250022, People's Republic of China*
[50]*University of Manchester, Oxford Road, Manchester M13 9PL, United Kingdom*
[51]*University of Minnesota, Minneapolis, Minnesota 55455, USA*
[52]*University of Muenster, Wilhelm-Klemm-Str. 9, 48149 Muenster, Germany*
[53]*University of Oxford, Keble Rd, Oxford OX13RH, United Kingdom*
[54]*University of Science and Technology Liaoning, Anshan 114051, People's Republic of China*
[55]*University of Science and Technology of China, Hefei 230026, People's Republic of China*
[56]*University of South China, Hengyang 421001, People's Republic of China*
[57]*University of the Punjab, Lahore 54590, Pakistan*
[58a]*University of Turin, I-10125 Turin, Italy*
[58b]*University of Eastern Piedmont, I-15121 Alessandria, Italy*
[58c]*INFN, I-10125 Turin, Italy*
[59]*Uppsala University, Box 516, SE-75120 Uppsala, Sweden*
[60]*Wuhan University, Wuhan 430072, People's Republic of China*
[61]*Xinyang Normal University, Xinyang 464000, People's Republic of China*
[62]*Zhejiang University, Hangzhou 310027, People's Republic of China*
[63]*Zhengzhou University, Zhengzhou 450001, People's Republic of China*

We study the $e^+e^- \to \gamma\omega J/\psi$ process using 11.6 fb^{-1} e^+e^- annihilation data taken at center-of-mass energies from $\sqrt{s} = 4.008$ GeV to 4.600 GeV with the BESIII detector at the BEPCII storage ring. The $X(3872)$ resonance is observed for the first time in the $\omega J/\psi$ system with a significance of more than 5σ. The relative decay ratio of $X(3872) \to \omega J/\psi$ and $\pi^+\pi^- J/\psi$ is measured to be $\mathcal{R} = 1.6^{+0.4}_{-0.3} \pm 0.2$, where the first uncertainty is statistical and the second systematic (the same hereafter). The $\sqrt{s}$-dependent cross section of $e^+e^- \to \gamma X(3872)$ is also measured and investigated, and it can be described by a single Breit-Wigner resonance, referred to as the $Y(4200)$, with a mass of $4200.6^{+7.9}_{-13.3} \pm 3.0$ MeV/c^2 and a width of $115^{+38}_{-26} \pm 12$ MeV. In addition, to describe the $\omega J/\psi$ mass distribution above 3.9 GeV/c^2, we need at least one additional Breit-Wigner resonance, labeled as $X(3915)$, in the fit. The mass and width of the $X(3915)$ are determined. The resonant parameters of the $X(3915)$ agree with those of the $Y(3940)$ in $B \to K\omega J/\psi$ and of the $X(3915)$ in $\gamma\gamma \to \omega J/\psi$ observed by the Belle and *BABAR* experiments within errors.

The $X(3872)$ resonance was first observed by the Belle experiment [1], and confirmed by the CDF [2], D0 [3], *BABAR* [4], LHCb [5], and BESIII Collaborations [6]. Its unusual properties do not accommodate with a charmonium state, and thus the $X(3872)$ resonance is widely explained as an unconventional meson candidate [7]. Since the $X(3872)$ mass is near the $\bar{D}^0 D^{*0}$ mass threshold, it is often interpreted as a hadronic molecule by theoretical models [8]. The hadronic molecule model predicts that the decay of $X(3872) \to \omega J/\psi$ is sensitive to its internal structure, and a precise measurement of the decay rate would help to determine the ratio of various components that contribute to the $X(3872)$ wave function. While the decay $X(3872) \to \pi^+\pi^- J/\psi$, where $\pi^+\pi^-$ is found to be dominated by a ρ^0 [9], violates the isospin symmetry in the strong interaction, the $X(3872) \to \omega J/\psi$ decay process conserves isospin symmetry, and thus such a decay provides an excellent metric for probing its isospin-violation effect. Previously, the Belle and *BABAR* Collaborations only reported less than 5σ evidences for the $X(3872) \to \omega J/\psi$ decay [10]. A solid observation is still lacking and is necessary for improved interpretation of this first experimentally observed state potentially composed of four quarks.

The BESIII Collaboration recently reported evidence for the radiative transition $Y(4260) \to \gamma X(3872)$ in $X(3872) \to \pi^+\pi^- J/\psi$ mode [6]. A charged charmoniumlike state $Z_c(3900)$, which is a good candidate for a four-quark state [11], was observed near $\sqrt{s} = 4.26$ GeV by BESIII [12] and Belle [13], and later confirmed with CLEO-c's data at

$\sqrt{s} = 4.17$ GeV [14]. All these observations show potential connections among the $X(3872)$, $Y(4260)$, and $Z_c(3900)$ resonances, and strongly hint towards a common underlying nature for them. At the moment, more supportive experimental observation for the transition process $Y(4260) \to \gamma X(3872)$ is needed to establish these connections.

The $Y(3940)$ resonance was observed by the Belle Collaboration [15] and confirmed by the *BABAR* Collaboration [16] in $B \to K\omega J/\psi$. Later on, both Belle and *BABAR* reported observations of the $X(3915)$ resonance in $\gamma\gamma \to \omega J/\psi$ process [17], and it was suggested to be the same resonance as the $Y(3940)$ by the Particle Data Group (PDG) [18]. The underlying nature of the $X(3915)$ is still unclear. It was once considered as a candidate for the $\chi_{c0}(2P)$ charmonium state. However, such kind of assignment was challenged by a recent Belle observation [19]. Other interpretations, such as a tetraquark [20] or a hadronic molecule [21] are proposed for the $X(3915)$. Moreover, a theoretical calculation predicted a 1^{++} tetraquark with mass near 3.95 GeV/c^2 [22]. To make the situation more clear, it is important to provide additional data on the $X(3915)$.

In this Letter, we report the study of the process $e^+e^- \to \gamma\omega J/\psi$, with $J/\psi \to \ell^+\ell^-$ ($\ell = e, \mu$) and $\omega \to \pi^+\pi^-\pi^0(\pi^0 \to \gamma\gamma)$, using data samples collected with the BESIII detector [23]. We search for the $X(3872)$ and $X(3915)$ resonances in the $\omega J/\psi$ system and study the $\sqrt{s}$-dependent production cross section, $\sigma[e^+e^- \to \gamma X(3872)]$. The e^+e^- center-of-mass (c.m.) energies of the data sets range from $\sqrt{s} = 4.008$ to 4.600 GeV (c.f. Supplemental Material [24]), with a total integrated luminosity of about 11.6 fb^{-1}.

The BESIII detector is described in detail elsewhere [23,25]. GEANT4 [26] based Monte Carlo (MC) simulation samples are used to optimize the event selection criteria, determine the detection efficiency, and estimate backgrounds. For the signal process, we generate $e^+e^- \to \gamma X(3872)/X(3915) \to \gamma\omega J/\psi$ MC events, with $J/\psi \to \ell^+\ell^-$ ($\ell = e, \mu$) and $\omega \to \pi^+\pi^-\pi^0(\pi^0 \to \gamma\gamma)$ at each c.m. energy corresponding to data. The $X(3872)/X(3915) \to \omega J/\psi$ decay is described with the phase-space model from EVTGEN [27]. Initial state radiation (ISR) is simulated with KKMC [28]. The maximum ISR photon energy is set to correspond to the 3.90 GeV/c^2 production threshold of the $\gamma X(3872)$ system. The final state radiation (FSR) from charged final-state particles are handled with PHOTOS [29].

Events with four charged tracks with net zero charge are selected. For each charged track, the polar angle in the multilayer drift chamber must satisfy $|\cos\theta| < 0.93$, and the point of closest approach to the e^+e^- interaction point must be within ± 10 cm in the beam direction and within 1 cm in the plane perpendicular to the beam direction. Since the $\pi^\pm$ from ω decay and $\ell^\pm$ from J/ψ decay are kinematically well separated, charged tracks with momenta larger than 1.0 GeV/c in the laboratory frame are assumed to be $\ell^\pm$, and the ones with momenta less than 1.0 GeV/c are assumed to be $\pi^\pm$. The energy deposition of charged tracks in the electromagnetic calorimeter (EMC) is used to separate e and μ. For $\mu^\pm$ candidates, the deposited energy in the EMC are required to be less than 0.35 GeV, while for $e^\pm$ it is required to be larger than 1.1 GeV.

Showers identified as good photon candidates must satisfy fiducial and shower-quality requirements. The minimum EMC energy is 25 MeV for barrel showers ($|\cos\theta| < 0.80$) and 50 MeV for end cap showers ($0.86 < |\cos\theta| < 0.92$). To eliminate showers produced by charged particles, a photon must be separated by at least 20 degrees from any charged track in the EMC. The time information from the EMC is also used to suppress electronic noise and energy deposits unrelated to the event. At least three good photon candidates are required in each event.

To improve the momentum and energy resolutions and to reduce backgrounds, a five-constraint (5C) kinematic fit is applied to an event with the hypothesis $e^+e^- \to \gamma\pi^+\pi^-\pi^0\ell^+\ell^-$, which constrains the sum of four momentum of the final-state particles to the initial colliding beams, and the mass of two photon combinations to the π^0 world average mass [18]. The χ^2 over number of degree of freedom (ndf) of the kinematic fit is required to be less than 100/5. When there are ambiguities due to multicombinations or multiphoton candidates in one event, we choose the combination with the smallest χ^2.

Background events such as $e^+e^- \to \pi^+\pi^-\psi(3686)/$ $\pi^0\pi^0\psi(3686) \to \pi^+\pi^-\pi^0\pi^0 J/\psi$ with one photon candidate missing would also pass the previously described event selection. To remove these backgrounds, we require $|M^{\text{recoil}}(\pi^+\pi^-) - m[\psi(3686)]| > 8$ MeV/c^2 and $|M(\pi^+\pi^- J/\psi) - m[\psi(3686)]| > 7$ MeV/c^2, where $M^{\text{recoil}}(\pi^+\pi^-) = \sqrt{(P_{e^+e^-} - P_{\pi^+\pi^-})^2}$, and $m[\psi(3686)]$ is the mass of the $\psi(3686)$ according to Ref. [18]. Other background events, such as $e^+e^- \to \eta' J/\psi \to \gamma\omega J/\psi$, have the same event topology as the signal. Their contribution can be effectively vetoed by rejecting events satisfying both $0.93 < M(\gamma\omega) < 0.97$ GeV/c^2 and $M(\omega J/\psi) > 3.9$ GeV/c^2.

After imposing the above requirements, clear peaks from J/ψ and ω decays are seen in the $\ell^+\ell^-$ and $\pi^+\pi^-\pi^0$ invariant mass distributions, as shown in Fig. 1. The η peak in the right panel of Fig. 1 comes from $e^+e^- \to \eta J/\psi$ and $\gamma_{\text{ISR}}\psi(3686) \to \gamma_{\text{ISR}}\eta J/\psi$ processes. To identify signal candidates that involve the J/ψ resonances, we select events within an invariant mass window of $3.07 < M(\ell^+\ell^-) < 3.14$ GeV/c^2, referred to as the J/ψ-mass window. Non-J/ψ background events are selected within the two sidebands $2.97 < M(\ell^+\ell^-) < 3.04$ GeV/c^2 or $3.17 < M(\ell^+\ell^-) < 3.24$ GeV/c^2.
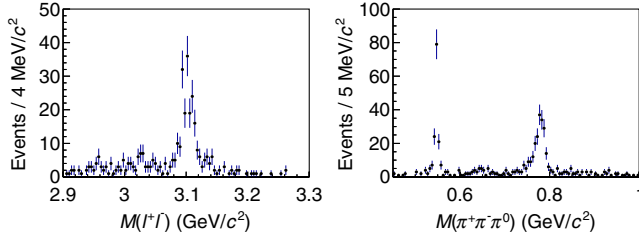
FIG. 1. The $M(\ell^+\ell^-)$ and $M(\pi^+\pi^-\pi^0)$ distributions from the full data sets.

The difference between the mass of $X(3872)$ and J/ψ [18] is about 775 MeV/c^2, which is slightly lower than the world average mass of the ω. A consequence is an asymmetric $M(\pi^+\pi^-\pi^0)$ distribution around the ω resonance, as can be seen in the right panel of Fig. 1. To accommodate for this effect, the ω mass window is defined as $0.72 < M(\pi^+\pi^-\pi^0) < 0.81$ GeV/c^2, and its mass sideband as $0.61 < M(\pi^+\pi^-\pi^0) < 0.70$ GeV/c^2 or $0.83 < M(\pi^+\pi^-\pi^0) < 0.92$ GeV/c^2. We fitted both the $M(\ell^+\ell^-)$ and $M(\pi^+\pi^-\pi^0)$ distributions, and normalized the data of the sidebands according to the fit results.

Figure 2 shows the $M(\omega J/\psi)$ [30] distribution from the full data set. A signal peak consistent with the $X(3872)$ resonance is observed. In addition, there are evident structures above 3.9 GeV/c^2. There are irreducible $e^+e^- \to \omega\chi_{c0}$ background events that produce a broad structure in the $M(\omega J/\psi)$ distribution. Such kind of
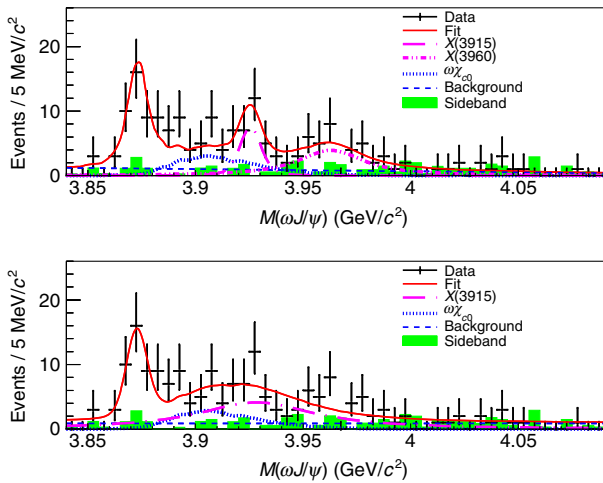

FIG. 2. The $M(\omega J/\psi)$ distribution with results of an unbinned maximum-likelihood fit to data including three BW resonances (upper) and including two BW resonances (bottom) as signal. Dots with error bars are data, the red solid curves show the total fit results, the blue dotted curves are the MC simulated $\omega\chi_{c0}$ background component, the blue dashed curves are the linear background component, the pink dotted-dashed curves are the $X(3915)$ resonance, the pink double-dotted dashed curve is the $X(3960)$ resonance, and the green shaded histograms are the normalized contribution from the J/ψ- and ω-mass sidebands.

background is well understood and can be reproduced by the MC simulation at BESIII [31]. Other possible backgrounds come from continuum events, such as $e^+e^- \to \gamma\omega\pi^+\pi^-$, $\gamma\pi^+\pi^-\pi^0 J/\psi$, $\gamma\pi^+\pi^-\pi^0\pi^+\pi^-$ etc. They are estimated by analyzing the J/ψ and ω mass sidebands data.

An unbinned maximum-likelihood fit is performed to the $M(\omega J/\psi)$ mass distribution. In the fit, we use as the signal probability density function (PDF) the incoherent sum of three Breit-Wigner (BW) resonances [denoted as $X(3872)$, $X(3915)$, and $X(3960)$, respectively], each convolved with a Gaussian resolution function. The $X(3872)$ width is set to 1.2 MeV [18]. The shape and yield of the $e^+e^- \to \omega\chi_{c0}$ background component are fixed to the results of the MC simulation. Contribution from other backgrounds is parameterized as a linear shape. The upper panel of Fig. 2 shows the fit results (numerical results are listed in Table I), and the extracted $X(3872)$ mass agrees with its world average value within errors. The obtained $X(3872)$ signal events yield is $N_{sig} = 45 \pm 9 \pm 3$. The statistical significance of the $X(3872)$ resonance is estimated to be 5.7σ by comparing the likelihood difference with or without the $X(3872)$ in the fit, $\Delta(-2\ln\mathcal{L}) = 40.8$, and by taking the change of ndf (Δndf $= 3$) into account. Possible systematic effects on the $X(3872)$ signal significance, including background shape, $\omega\chi_{c0}$ background normalization, $X(3872)$ intrinsic width and mass resolution are investigated, and no sign for a decreased $X(3872)$ significance is observed. The statistical significance of $X(3915)$ and $X(3960)$ are estimated to be 3.1σ and 3.4σ only.

As an alternative choice, we fit the $M(\omega J/\psi)$ mass distribution only with the $X(3872)$ and $X(3915)$ resonances as signal PDF. The $e^+e^- \to \omega\chi_{c0}$ background is handled in the same way as before. The contribution from other backgrounds is parametrized as a linear function and has been fixed as the result of fitting it to the data of the J/ψ- and ω-mass sidebands. The bottom panel of Fig. 2 shows the fit results (c.f. Table I), and the number of fitted $X(3872)$ signal events is $N_{sig} = 40 \pm 8 \pm 3$. The statistical significance of $X(3872)$ is estimated to be 5.2σ, and found to be larger than 5.1σ after considering systematic effects from $\omega\chi_{c0}$ and linear background normalization, $X(3872)$ intrinsic width and mass resolution. The statistical significance of $X(3915)$ is estimated to be 6.9σ. We test the

TABLE I. The masses (in MeV/c^2) and widths (in MeV) of the $X(3872)$, $X(3915)$, and $X(3960)$ resonances from the fit. The numbers in brackets represent the fit scenario without the $X(3960)$. The uncertainties are statistical only.

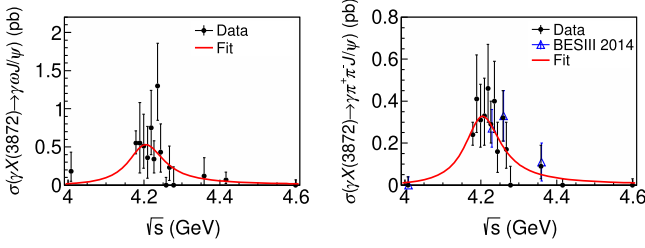|	Mass	Width
$X(3872)$	$3873.3 \pm 1.1 (3872.8 \pm 1.2)$	$1.2(1.2)$
$X(3915)$	$3926.4 \pm 2.2 (3932.6 \pm 8.7)$	$3.8 \pm 7.5 (59.7 \pm 15.5)$
$X(3960)$	3963.7 ± 5.5	33.3 ± 34.2

FIG. 3. The measured cross section of $\sigma[e^+e^- \to \gamma X(3872)]$ times the branching fraction of $X(3872) \to \omega J/\psi$ (left) and $\pi^+\pi^- J/\psi$ (right), and a simultaneous fit to data with a single BW resonance. Dots with error bars are data, the open triangles are an early measurement reported in Ref. [6], and the red curves show the fit results.

significance between these two fit scenarios, and find they only differ by 2.5σ.

The production cross section of $e^+e^- \to \gamma X(3872)$ times the branching fraction $\mathcal{B}[X(3872) \to \omega J/\psi]$ at each c.m. energy is calculated as $\sigma\mathcal{B}[X(3872) \to \omega J/\psi] = [N^{\rm sig}/\mathcal{L}\epsilon(1+\delta)\mathcal{B}]$, where $N^{\rm sig}$ is the number of $X(3872)$ signal events, $\mathcal{L}$ is the integrated luminosity, ϵ is the detection efficiency, $\mathcal{B}$ is the product of branching fractions for $J/\psi \to \ell^+\ell^-$ and $\omega \to \pi^+\pi^-\pi^0(\pi^0 \to \gamma\gamma)$, and $1+\delta$ is the ISR radiative correction factor, which is calculated using the KKMC program [28]. The ISR photon energy distribution is obtained by an iterative procedure using the line shape $\sigma[e^+e^- \to \gamma X(3872)]$ measured in this study to replace the default one of KKMC. The left panel of Fig. 3 shows the measured $\sigma\mathcal{B}[X(3872) \to \omega J/\psi]$. Using the same analysis method as described in Ref. [6] and the radiative correction factor in this study, $\sigma\mathcal{B}[X(3872) \to \pi^+\pi^- J/\psi]$ is measured as well. Our result agrees with and supersedes the earlier published BESIII measurement [6], as shown in the right panel of Fig. 3. All the numerical results can be found in the Supplemental Material [24].

A simultaneous maximum-likelihood fit is performed to both the $\sigma\mathcal{B}[X(3872) \to \omega J/\psi]$ and the $\sigma\mathcal{B}[X(3872) \to \pi^+\pi^- J/\psi]$ distributions. We use a single BW resonance, denoted as $Y(4200)$, with free mass and width as PDF. A free parameter $\mathcal{R} = \{\mathcal{B}[X(3872) \to \omega J/\psi]/\mathcal{B}[X(3872) \to \pi^+\pi^- J/\psi]\}$ is used to describe the relative decay rate of $X(3872) \to \omega J/\psi$ and $\pi^+\pi^- J/\psi$, which is common for every c.m. energy. The fit gives $M[Y(4200)] = 4200.6^{+7.9}_{-13.3}$ MeV/c^2, $\Gamma[Y(4200)] = 115^{+38}_{-26}$ MeV, $\Gamma^{ee} \cdot \mathcal{B}[Y(4200) \to \gamma X(3872)]\mathcal{B}[X(3872) \to \pi^+\pi^- J/\psi] = (4.5^{+1.1}_{-0.8}) \times 10^{-2}$ eV and $\mathcal{R} = 1.6^{+0.4}_{-0.3}$, where Γ^{ee} is the electronic partial width of the $Y(4200)$. Here, all the uncertainties are statistical only.

The systematic uncertainty for $X(3872)$, $X(3915)$, and $X(3960)$ mass and width measurements come from the uncertainties in the absolute mass scale, background, and resolution effects. The $e^+e^- \to \gamma_{\rm ISR}\psi(3686) \to \gamma_{\rm ISR}\eta J/\psi$ events with the same event selection (except the ω mass

window is replaced by the η mass window) are used as a control sample to calibrate the mass scale. The measured $\psi(3686)$ mass is 3685.4 ± 0.4 MeV/c^2, and the difference to the $\psi(3686)$ world average mass is 0.8 MeV/c^2. Backgrounds are varied from a linear shape to a second-order polynomial or by $\pm 1\sigma$ for the linear component, and varied by $\pm 1\sigma$ for the $\omega\chi_{c0}$ component in the fit. The differences in the mass and width measurements with respect to the nominal results are taken as a systematic uncertainty. The systematic uncertainty of resolution is estimated by varying the Gaussian parameters of the resolution response function by $\pm 1\sigma$ in the signal PDF. In both fit scenarios [with and without the $X(3960)$], the $X(3872)$ mass difference 0.5 MeV/c^2 is taken as a systematic uncertainty due to the fit model. All these contributions are summarized in Table II, and the total uncertainty is calculated by adding the independent contributions in quadrature.

The systematic uncertainty for the $e^+e^- \to \gamma X(3872)$ cross section measurement mainly comes from uncertainties in the luminosity measurements, detection efficiency, signal extraction, radiative correction, and branching fractions. The integrated luminosities of each data set are measured with large-angle Bhabha scattering events, with an uncertainty of 1.0% [32]. The tracking efficiency is estimated to be 1% per track from a study of the control sample $J/\psi \to p\bar{p}\pi^+\pi^-$. The uncertainty due to the photon reconstruction is studied using the $J/\psi \to \pi^+\pi^-\pi^0$ events, and is found to be 1% for the radiative photon [33]. An additional systematic uncertainty of 1% is assigned to the efficiency of π^0 reconstruction by studying $\psi(3686) \to \pi^0\pi^0 J/\psi$ and $e^+e^- \to \omega\pi^0$ events. In our event selection, a 5C kinematic fit is used, and the systematic uncertainty related to the kinematic fit is estimated to be 0.8% by using a helix correction method as discussed in Ref. [34].

The number of $X(3872)$ signal events is extracted by fitting the $M(\omega J/\psi)$ distribution, and the difference between the two fit scenarios is 9.5%. The $X(3872)$ intrinsic width is fixed to 1.2 MeV in the signal PDF. Varying the width from 50 keV to 1.2 MeV results in a 5% difference for the $X(3872)$ signal yield. The systematic uncertainty of the $\omega\chi_{c0}$ background is estimated by varying

TABLE II. Summary of the systematic uncertainties for $X(3872)/X(3915)/X(3960)$ mass and width measurements. The numbers in the brackets correspond to the fit scenario with only the $X(3872)$ and $X(3915)$ as signal PDF.

Source	Mass (MeV/c^2)	Width (MeV)
Absolute mass scale	0.8/0.8 (0.8)/0.8	$\cdots$/$\cdots$/$\cdots$
Background shape	0.3/0.4 (4.5)/0.5	$\cdots$/2.5 (3.6)/8.3
Resolution	0.0/0.8 (0.7)/0.8	$\cdots$/0.7 (0.3)/0.1
Fit model	0.5/$\cdots$/$\cdots$	$\cdots$/$\cdots$/$\cdots$
Total	1.0/1.2 (4.7)/1.3	$\cdots$/2.6 (3.7)/8.3

the normalization by $\pm 1\sigma$, which will cause a difference of 0.9% in the $X(3872)$ signal yield. The remaining background is parameterized as a linear function. Varying the background shape from linear to a second-order polynomial or the normalization by $\pm 1\sigma$ will cause a 3.1% difference for the $X(3872)$ signal yield.

We iterate the cross section measurement until the value of $(1 + \delta)\epsilon$ changes by at most 1% from the previous iteration, and 1% is taken as a systematic uncertainty due to ISR radiative correction. The systematic uncertainty related to the J/ψ-mass window cut is 1.6% [6]. The branching fraction uncertainties of $J/\psi \to \ell^+\ell^-$, $\omega \to \pi^+\pi^-\pi^0$ and $\pi^0 \to \gamma\gamma$ are 0.6%, 0.8%, and 0.04% [18], respectively.

The total systematic uncertainty is calculated to be 12.3% by adding all contributions in quadrature.

The systematic uncertainty for the $Y(4200)$ parameters mainly comes from the uncertainties related to the e^+e^- c.m. energy measurement, the parametrization of the fit model, and the cross section measurement. The c.m. energy of each data set is measured with dimuon events, with ± 0.8 MeV uncertainty [35]. Such kind of common uncertainty will shift the $Y(4200)$ line shape globally, and thus, propagate to the $Y(4200)$ mass linearly. In the fit to the cross section, the $Y(4200)$ resonance is parametrized as a BW with a constant full width. We also use a BW with a phase-space dependent full width, $\Gamma[\Phi(\sqrt{s})/\Phi(M)]$, and the difference is 2.8 MeV/c^2 for the mass, 12 MeV for the width, and 6.5% for Γ^{ee}. The cross section data measured in $X(3872) \to \omega J/\psi$ and $\pi^+\pi^- J/\psi$ channels are fitted simultaneously. The common uncertainties of cross section measurements in both channels, including luminosity, tracking, photon detection, radiative correction, kinematic fit, $X(3872)$ intrinsic width, J/ψ mass window, and $J/\psi \to \ell^+\ell^-$ branching fraction, will propagate to Γ^{ee} linearly, i.e., 6.9%. The uncommon ones, including π^0, background, fit model, and $\omega \to \pi^+\pi^-\pi^0(\pi^0 \to \gamma\gamma)$ branching fraction, will affect the $\mathcal{R}$ measurement, and the total contribution is 10.9%, by adding them in quadrature.

In summary, we have studied the $e^+e^- \to \gamma\omega J/\psi$ process with 11.6 fb^{-1} data at the BESIII experiment. For the first time, the $X(3872) \to \omega J/\psi$ decay was firmly observed with more than 5σ significance, and the $X(3872)$ mass was measured to be $3873.3 \pm 1.1 \pm 1.0$ MeV/c^2. The relative decay ratio for $X(3872) \to \omega J/\psi$ and $\pi^+\pi^- J/\psi$ is measured to be $\mathcal{R} = 1.6^{+0.4}_{-0.3} \pm 0.2$, which agrees well with previous measurements within errors [10]. These measurements provide important input for the hadronic molecule interpretation for the $X(3872)$ resonance [8].

To describe the $M(\omega J/\psi)$ distribution above 3.9 GeV/c^2, we need at least one additional BW resonance $X(3915)$. Its mass and width are measured to be $3926.4 \pm 2.2 \pm 1.2$ MeV/c^2 and $3.8 \pm 7.5 \pm 2.6$ MeV, or $3932.6 \pm 8.7 \pm 4.7$ MeV/c^2 and $59.7 \pm 15.5 \pm 3.7$ MeV, depending on the fit models.

The $e^+e^- \to \gamma X(3872)$ production cross section is measured at the c.m. energies between 4.008 and 4.600 GeV [24]. We studied the $\sqrt{s}$-dependent cross section line shape of $e^+e^- \to \gamma X(3872)$, and find it can be described by a single BW resonance $Y(4200)$. A simultaneous fit to the $X(3872) \to \omega J/\psi$ and $\pi^+\pi^- J/\psi$ cross section data gives its mass $M[Y(4200)] = 4200.6^{+7.9}_{-13.3} \pm 3.0$ MeV/c^2, and width $\Gamma[Y(4200)] = 115^{+38}_{-26} \pm 12$ MeV, which agree with the $\psi(4160)$ [18] or the $Y(4220)$ observed by BESIII in $\pi^+\pi^- J/\psi$ [36] and $\pi^+\pi^- h_c$ [37] within errors. The measured $e^+e^- \to \gamma X(3872)$ cross section provides useful information for the $D\bar{D}^*$ hadronic molecule calculation as described in Ref. [38].

[*]Corresponding author.
z.liu@sdu.edu.cn
[a]Also at Bogazici University, 34342 Istanbul, Turkey.
[b]Also at the Moscow Institute of Physics and Technology, Moscow 141700, Russia.
[c]Also at the Functional Electronics Laboratory, Tomsk State University, Tomsk 634050, Russia.
[d]Also at the Novosibirsk State University, Novosibirsk 630090, Russia.

[e]Also at the NRC "Kurchatov Institute", PNPI, 188300 Gatchina, Russia.

[f]Also at Istanbul Arel University, 34295 Istanbul, Turkey.

[g]Also at Goethe University Frankfurt, 60323 Frankfurt am Main, Germany.

[h]Also at Key Laboratory for Particle Physics, Astrophysics and Cosmology, Ministry of Education; Shanghai Key Laboratory for Particle Physics and Cosmology; Institute of Nuclear and Particle Physics, Shanghai 200240, People's Republic of China.

[i]Also at Government College Women University, Sialkot 51310, Punjab, Pakistan.

[j]Also at Key Laboratory of Nuclear Physics and Ion-beam Application (MOE) and Institute of Modern Physics, Fudan University, Shanghai 200443, People's Republic of China.

[k]Also at Harvard University, Department of Physics, Cambridge, Massachusetts 02138, USA.

[1] S. K. Choi *et al.* (Belle Collaboration), Phys. Rev. Lett. **91,** 262001 (2003).

[2] D. Acosta *et al.* (CDF Collaboration), Phys. Rev. Lett. **93,** 072001 (2004).

[3] V. M. Abazov *et al.* (D0 Collaboration), Phys. Rev. Lett. **93,** 162002 (2004).

[4] B. Aubert *et al.* (*BABAR* Collaboration), Phys. Rev. D **71,** 071103 (2005).

[5] R. Aaij *et al.* (LHCb Collaboration), Eur. Phys. J. C **72,** 1972 (2012); Phys. Rev. Lett. **110,** 222001 (2013).

[6] M. Ablikim *et al.* (BESIII Collaboration), Phys. Rev. Lett. **112,** 092001 (2014).

[7] N. Brambilla *et al.*, Eur. Phys. J. C **71,** 1534 (2011); H. X. Chen, W. Chen, X. Liu, and S. L. Zhu, Phys. Rep. **639,** 1 (2016); S. Lars Olsen, T. Skwarnicki, and D. Zieminska, Rev. Mod. Phys. **90,** 015003 (2018).

[8] E. S. Swanson, Phys. Lett. B **588,** 189 (2004); F.-K. Guo, C. Hanhart, U.-G. Meißner, Q. Wang, Q. Zhao, and B.-S. Zou, Rev. Mod. Phys. **90,** 015004 (2018).

[9] A. Abulencia *et al.* (CDF Collaboration), Phys. Rev. Lett. **96,** 102002 (2006).

[10] P. del Amo Sanchez *et al.* (*BABAR* Collaboration), Phys. Rev. D **82,** 011101(R) (2010); K. Abe *et al.* (Belle Collaboration), arXiv:hep-ex/0505037.

[11] E. Swanson, Physics **6,** 69 (2013).

[12] M. Ablikim *et al.* (BESIII Collaboration), Phys. Rev. Lett. **110,** 252001 (2013).

[13] Z. Q. Liu *et al.* (Belle Collaboration), Phys. Rev. Lett. **110,** 252002 (2013).

[14] T. Xiao, S. Dobbs, A. Tomaradze, and K. K. Seth, Phys. Lett. B **727,** 366 (2013).

[15] S. K. Choi *et al.* (Belle Collaboration), Phys. Rev. Lett. **94,** 182002 (2005).

[16] B. Aubert *et al.* (*BABAR* Collaboration), Phys. Rev. Lett. **101,** 082001 (2008).

[17] S. Uehara *et al.* (Belle Collaboration), Phys. Rev. Lett. **104,** 092001 (2010); J. P. Lees *et al.* (*BABAR* Collaboration), Phys. Rev. D **86,** 072002 (2012).

[18] M. Tanabashi *et al.* (Particle Data Group), Phys. Rev. D **98,** 030001 (2018).

[19] K. Chilikin *et al.* (Belle Collaboration), Phys. Rev. D **95,** 112003 (2017).

[20] R. F. Lebed and A. D. Polosa, Phys. Rev. D **93,** 094024 (2016).

[21] X. Li and M. B. Voloshin, Phys. Rev. D **91,** 114014 (2015).

[22] J. Wu, X. Liu, Y. R. Liu, and S. L. Zhu, Phys. Rev. D **99,** 014037 (2019).

[23] M. Ablikim *et al.* (BESIII Collaboration), Nucl. Instrum. Methods Phys. Res., Sect. A **614,** 345 (2010).

[24] See Supplemental Material at http://link.aps.org/supplemental/10.1103/PhysRevLett.122.232002 for a summary of $\sqrt{s}$, integrated luminosity, detection efficiencies, ISR radiative correction factor, the numbers of signal events, and cross sections at each c.m. energy.

[25] X. Li *et al.*, Radiat. Detect. Technol. Methods **1,** 13 (2017); Y. X. Guo *et al.*, *ibid.* **1,** 15 (2017).

[26] S. Agostinelli *et al.* (GEANT4 Collaboration), Nucl. Instrum. Methods Phys. Res., Sect. A **506,** 250 (2003).

[27] D. J. Lange, Nucl. Instrum. Methods Phys. Res., Sect. A **462,** 152 (2001).

[28] S. Jadach, B. F. L. Ward, and Z. Was, Comput. Phys. Commun. **130,** 260 (2000); Phys. Rev. D **63,** 113009 (2001).

[29] P. Golonka and Z. Was, Eur. Phys. J. C **45,** 97 (2006).

[30] Here $M(\omega J/\psi) = M(\pi^+\pi^-\pi^0\ell^+\ell^-) - M(\ell^+\ell^-) + m(J/\psi)$ is used to partially cancel the mass resolution of the lepton pair, and $m(J/\psi)$ is the nominal mass of J/ψ [18].

[31] M. Ablikim *et al.* (BESIII Collaboration), Phys. Rev. Lett. **114,** 092003 (2015); Phys. Rev. D **99,** 091103 (2019).

[32] M. Ablikim *et al.* (BESIII Collaboration), Chin. Phys. C **39,** 093001 (2015).

[33] M. Ablikim *et al.* (BESIII Collaboration), Phys. Rev. D **81,** 052005 (2010).

[34] M. Ablikim *et al.* (BESIII Collaboration), Phys. Rev. D **87,** 012002 (2013).

[35] M. Ablikim *et al.* (BESIII Collaboration), Chin. Phys. C **40,** 063001 (2016).

[36] M. Ablikim *et al.* (BESIII Collaboration), Phys. Rev. Lett. **118,** 092001 (2017).

[37] M. Ablikim *et al.* (BESIII Collaboration), Phys. Rev. Lett. **118,** 092002 (2017).

[38] F.-K. Guo, C. Hanhart, U.-G. Meißner, Q. Wang, and Q. Zhao, Phys. Lett. B **725,** 127 (2013).